10

Highly Doped Nd:YAG Laser in Bounce Geometry Under Quasi-Continuous Diode Pumping

Michal Jelínek and Václav Kubeček
Czech Technical University in Prague
Czech Republic

1. Introduction

Nanosecond and picosecond laser pulses play increasing role in a variety of applications, such as microsurgery, micromachining, ranging, optical parametric amplifiers pumping, remote sensing, nonlinear optics, etc. Efficient diode pumped solid state lasers represent widely used sources of such pulses. For applications such as laser ranging and some nonlinear optical effects investigation, the extremely short pulses are not needed and pulses in the range from tens of picoseconds to units of nanoseconds at repetition rates below 1 kHz are optimal. Research and development of such laser systems is the subject of this chapter.

In the diode pumped solid state laser technique several resonator configurations and pumping schemes are utilized. One of interesting setups with unique properties is bounce geometry resonator configuration (Alcock, 1997) when a slab active material is used and the laser beam experiences total internal reflection and amplification on the pumped crystal side. This arrangement has several advantages. The slab crystal shape allows good heat dissipation, because it is relatively thin and can be cooled from one or both sides. As a pump source, high power laser diode single bar or bar stacks can be used without bulky additional optics or radiation delivery fibers. In addition, laser resonator mode can be optimized to match the pumped region profile. Efficient operation of the bounce geometry laser pumped by the laser diode bar requires active medium with a high absorption coefficient for the pump radiation in order to obtain thin region with high gain near the pumping side. Therefore, materials as Nd:$GdVO_4$ and Nd:YVO_4 has challenged Nd:YAG with standard doping concentration of around 1 at.%. When recently Nd:YAG laser crystals with higher doping level (more than 2 at.%) became available (Urata, 2001), efficient operation of these crystals under bounce geometry has been demonstrated operating at 1.06 and 1.3 μm (Sauder, 2006; 2007). Nd:YAG crystals have better thermal and mechanical properties, and better energy storage capacity due to the longer upper state life-time in comparison with vanadates giving potential to generate more energetic pulses in the Q-switched and mode-locked regime.

Highly-energetic pulses in the nanosecond range can be obtained from the oscillator using active or passive Q-switching, which is well-known and widespread technique, mostly used under continuous pumping. In order to obtain more energetic pulses, quasi-continuous (QCW) pumping can be employed. Using the 2 at.% Nd:YAG in bounce geometry under QCW pumping, passively Q-switched operation at 1.06 μm has been reported with maximum

output energy of 2.3 mJ in a 12 ns pulse (Sauder, 2006). At 1.3 μm, actively Q-switched operation with maximum pulse energy of 1.8 mJ in 50 ns pulse was produced (Sauder, 2007).

In order to generate pulses in the picosecond and sub-picosecond range, the laser has to be operated in the mode-locking (ML) regime. In the solid state lasers, mostly passive ML techniques are used. These techniques can be divided into several groups. One large group is based on saturable absorbers based on different materials and media. The next group of techniques involves usage of nonlinear effects of different orders. The second order nonlinearity is involved in nonlinear mirror ML (Stankov, 1988; Thomas, 2010) and the third order in Kerr-lens ML (Agnesi, 1994; Spence, 1991). In the case of saturable absorbers, the dye saturable absorber (Schafer, 1976) was widely used in the previous decades, but because of the dye long-term instability, toxicity, and difficult manipulation, it was in the last decade replaced by solid state saturable absorbers. With the semiconductor technique development, the possibility of fabrication of the semiconductor saturable absorber with requested parameters appeared. Such absorber is based on one or more quantum wells grown on the semiconductor substrate. At the wavelength of about 1 μm, the quantum well is usually formed by the InGaAs layer with the thickness of several nanometers surrounded by the GaAs layers. As the InGaAs energy band gap is lower than GaAs band gap, it serves as a quantum well. According to the number of quantum wells and other growing parameters, the resulting characteristics, such as modulation depth, relaxation time constant, and saturation fluence can be adjusted according to the required application and laser operation conditions. Such saturable absorber is placed into the resonator in the transmission mode, usually under the Brewster's angle to avoid refections from the GaAs with high-refractive index. Alternatively, the saturable absorber structure can be grown on the Bragg mirror forming so called semiconductor saturable absorber mirror (SAM), which is placed as a rear mirror in the laser resonator and which has been widely used (Keller, 1996). Use of SAM as the ML technique has also some disadvantages. At first the laser output power is limited by the SAM structure damage threshold. The output pulse duration is also limited by the SAM relaxation time constant. The another approach to the solid-state saturable absorber development utilizes carbon nanotubes or graphene. Mode-locking operation of Nd-doped solid state lasers using carbon nanotubes SA (Yim, 2008) or graphene SA (Lee, 2010; Tan, 2010) was recently demonstrated.

Using semiconductor SAM, the output train of low energy pulses usually under continuous pumping is produced. In order to obtain pulses with higher energy directly from the oscillator, the semiconductor saturable absorber containing multiple quantum wells with higher modulation depth can be used in the laser resonator under QCW pumping. Bounce geometry can be considered as a proper resonator configuration for efficient mode-locking operation in this pumping regime. Efficient operation of quasi-continuously pumped 1 at.% doped Nd:YAG (Kubeček, 2008) and also Nd:YVO_4 and Nd:$GdVO_4$ (Kubeček, 2009a; 2010) using the saturable absorber in the transmission mode was already reported.

For applications requiring more energetic pulses or higher average power, the laser oscillator output can be further amplified using a laser amplifier in various configurations involving regenerative amplifier (Luhrmann, 2009), zigzag slab geometry (Cui, 2009; Fu, 2010), multiple amplification media (Fu, 2009), or hybrid fiber and solid-state system (Wushouer, 2010). These configurations are usually based on Nd:YAG or Nd:YVO_4 active materials with concentrations below 1 at.%. Much simpler amplifier configuration providing high gain involve grazing incidence geometry based on 1 at.% Nd:YVO_4 slab crystal (Agnesi, 2008; 2010).

2. Nd:YAG crystal with doping concentration of 2.4 at.%

High neodymium concentration results in shorter upper-state (fluorescence) lifetime caused by concentration quenching. At the typical Nd concentration of 1 at.% the fluorescence lifetime is about 230 μs (Koechner, 2006). At the concentration of 2 at.% the lifetime shortening to 145 - 180 μs and further at 3 at.% to 120 - 130 μs (Dong, 2005; Urata, 2001) was reported.

In our experiments we have used a Nd:YAG slab crystal with dimensions of $30 \times 5 \times 2$ mm grown by Czochralski method with Nd concentration of 2.4 at.%. Two 5×2 mm end faces were angled at 68 degrees. This configuration allows the laser cavity beam to be incident at Brewster's angle to these faces and to experience total internal reflection from the diode pumped face which results in laser operation in the horizontally polarized state. The pumping face 30×2 mm was antireflection coated at the 808 nm pump wavelength.

As a pump source the linear single bar quasi-continuous diode array LD with the fast axis collimation, nominal output power of 180 W and repetition rate up to 100 Hz was used. This diode was mounted on the copper plate with Peltier cooling enabling fine generated radiation wavelength tuning around 808 nm to match the Nd:YAG absorption peak.

2.1 Nd^{3+} lifetime measurement

The integral fluorescence decay from our crystal for excitation at the wavelength of 808 nm was measured using a Si photodiode in the spectral region above 1000 nm and is shown in Fig. 1. Calculated lifetime of 135 μs is in the good agreement with other published results.

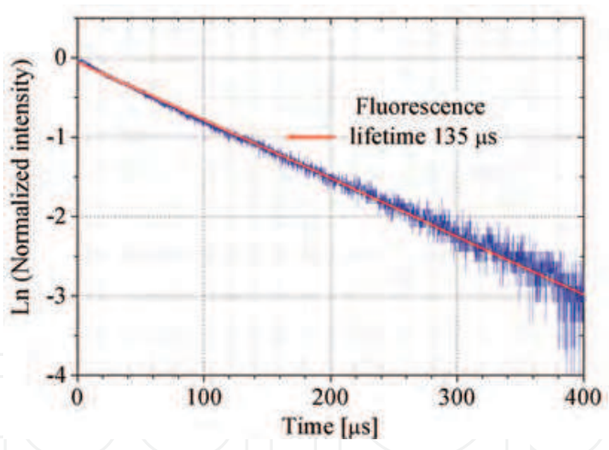

Fig. 1. Fluorescence lifetime measurement of 2.4 at.% Nd:YAG slab crystal.

3. Free-running laser operation at 1.06, 1.3 and 1.4 μm

The laser free-running operation was investigated at the output wavelengths of 1.06, 1.3, and 1.4 μm and is described in details in Kubeček (2009b). Schematic of the laser oscillator is shown in Fig. 2.

Generation at the wavelength of 1.06 μm was studied at first. The 17 cm long laser resonator was formed by a spherical high reflective mirror HR (radius of curvature of 300 mm) and a flat output coupler OC. Various OC reflectivities of 82, 50 and 30 % at 1.06 μm were tested.

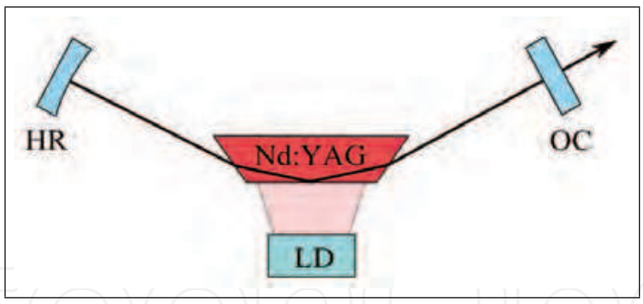

Fig. 2. Schematic of the Nd:YAG laser oscillator in bounce geometry operated in the free-running regime.

The Nd:YAG crystal was inserted approximately in the middle of the resonator. The output pulse energy with respect to the pump pulse energy is shown in Fig. 3. The pump pulse duration was set to 200 μs. For the output coupler with reflectivity of 82 % the slope efficiency of 50 % was obtained. The maximum output energy of 17 mJ for the pump energy of 38 mJ corresponds to the optical to the optical efficiency of 44.6 %. The output beam spatial profile was elliptical in the horizontal axis and is shown in the inset of Fig. 3 (for the output coupler reflectivity of 50 %).

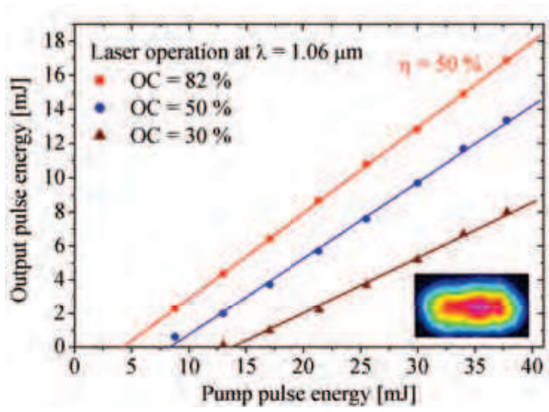

Fig. 3. The laser output characteristics in the free-running regime at 1.06 μm with various output couplers.

The slab shape with uncoated faces allowing the laser beam to be incident on the Nd:YAG at the Brewster's angle has the advantage in possibility of using the same crystal for generation at different wavelengths. We have successfully investigated efficient operation at 1.3 and 1.4 μm and the results were compared with values obtained for the generation at 1.06 μm. For the generation at 1.3 μm the HR mirror (radius of curvature of 150 mm) was highly reflective in this spectral region and had low reflectivity at 1.06 μm. The laser resonator was 95 mm long. For the generation at 1.4 μm the curvature of this mirror was the same, but the mirror was highly reflective at 1.4 μm. The output pulse energy with respect to the pump pulse energy is shown in Fig. 4. The maximum output energy at 1.3 μm was 8.5 mJ for the pump energy of 38 mJ and was obtained using the output coupler with reflectivity of 94 %. This corresponds to the optical to optical efficiency of 22.5 % and slope efficiency of 26 %.

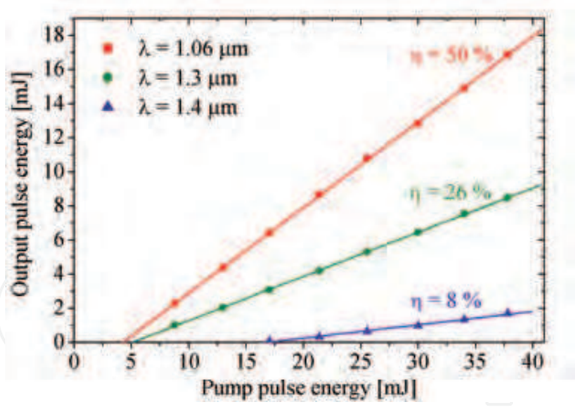

Fig. 4. Comparison of the laser operation at different wavelengths: 1.06, 1.3, and 1.4 μm.

The lowest curve in Fig. 4 shows the output pulse energy at 1.4 μm versus pump pulse energy. The maximum output energy of 1.5 mJ for the pump energy of 38 mJ was obtained using output coupler with reflectivity of 96 %. This corresponds to the optical to optical efficiency of 4.1 % and slope efficiency of 8.4 %.

4. Passively Q-switched laser operation at 1.06 and 1.3 μm

Q-switched laser operation was investigated at the output wavelengths of 1.06 and 1.3 μm and is described in details in Jelínek (2011a).

The laser resonator schematic was similar to that used in the free-running regime (shown in Fig. 2). At 1.06 μm the 80 mm long optical resonator was formed by a spherical high reflective mirror HR (radius of curvature of 300 mm) and a flat output coupler OC with reflectivity of 50 %. In order to obtain Q-switched regime, two 5 mm long anti-reflection (AR) coated Cr:YAG crystals with low signal transmission of 58 % (corresponding to the total low power transmission of 34 %) were introduced into the resonator close to the output coupler OC. Stable Q-switched operation was obtained for the pump energy of 17 mJ. The single 5 ns output pulse with energy of 1.3 mJ was generated directly from the oscillator and its oscillogram is shown in Fig. 5. The output beam spatial profile was Gaussian in both axes and is shown in the inset of the figure.

At 1.3 μm the 100 mm long optical resonator was formed by a spherical high reflective mirror HR (radius of curvature of 300 mm) and a flat output coupler OC with reflectivity of 70 % at 1.3 μm. Both dichroic mirrors have low reflectivity at wavelength of 1064 nm. As a saturable absorber V:YAG crystal with low signal transmission of 60 % and AR coating was used. Because of possible AR coating damage the saturable absorber was placed close to the rear high reflective mirror HR, where the fundamental laser mode radius is larger. Stable Q-switched operation at 1.3 μm was obtained for the pump energy of 30 mJ, which is nearly two times higher than the pump energy for the operation at 1.06 μm, caused by lower gain at 1.3 μm transition. Generation at the single wavelength of 1338 nm was confirmed by the spectrometer (Ocean Optics NIR512). The 13 ns output pulse with energy of 600 μJ was generated directly from the oscillator and its oscillogram is shown in Fig. 6. The output beam spatial profile shown in the inset of the figure was investigated by a standard silicon CCD

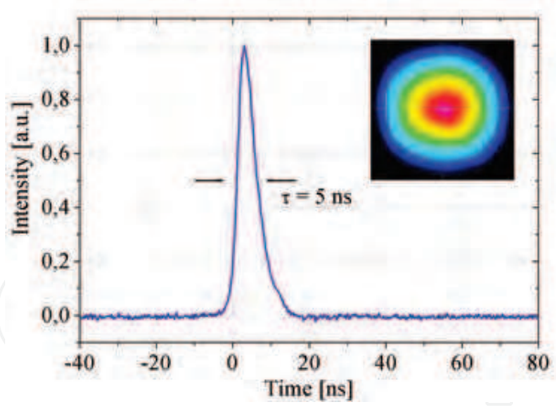

Fig. 5. Oscillogram of the Q-switched output pulse at 1.06 μm.

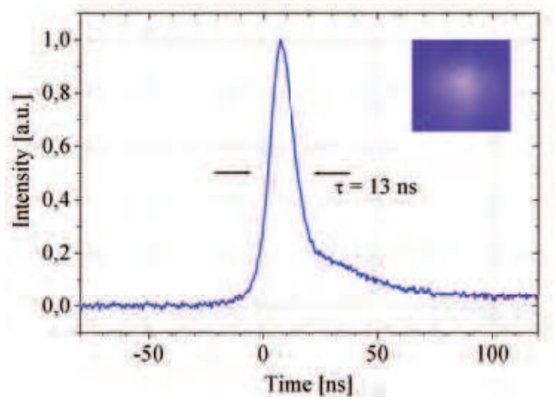

Fig. 6. Oscillogram of the Q-switched output pulse at 1.34 μm.

camera. Because of its low sensitivity in this region the measured signal was quite low but it can be deduced that the beam profile was approximately Gaussian in both axes.

5. Passively mode-locked laser operation at 1.06 μm

In order to obtain mode-locked laser operation, two types of semiconductor saturable absorbers (SA) were tested. In the first case the SA in the transmission mode was used and the output characteristics were compared with the characteristics of the laser mode-locked using the semiconductor saturable absorber mirror (SAM).

5.1 Laser mode-locking by saturable absorber in transmission mode

In the transmission mode two saturable absorbers were investigated in two resonator configurations. The saturable absorbers were grown by molecular beam epitaxy at the Center for High Technology Materials of the University of New Mexico (Diels, 2006; Kubeček, 2009c). The structures were grown on the 400 μm thick GaAs substrates and consisted of 33 or 100 quantum wells (QW) formed by the periods of 9 nm thick $In_{0.275}Ga_{0.725}As$ and 11 nm thick GaAs layers grown at low temperature (around 350° C) in order to decrease the carrier lifetime to the value less than 50 ps (Gupta, 1992). Number of the QWs determines the saturable absorber modulation depth and low-power transmission which were in the case of the SA

with 100 QW measured to be ∼25 % and ∼50 %, respectively. In the case of SA with 33 QW the modulation depth is lower. The GaAs substrate can be used also as a nonlinear element for passive negative feedback by beam defocusing (Corno, 1990; Diels, 2006). The laser resonators differ in length between 25 and 116 cm and also in the ratio of the beam radius inside the Nd:YAG crystal and on the SA. The experimental details are described in Jelínek (2010; 2011b).

5.1.1 Laser operation with short resonator

A schematic diagram of the mode-locked laser oscillator in the configuration (A) is shown in Fig. 7a. The 250 mm long laser resonator was formed by the spherical high reflective mirror HR (radius of curvature of 300 mm) and a flat output coupler OC with reflectivity of 30 %. The Nd:YAG crystal was inserted at a distance of 130 mm from the OC. The fundamental laser beam profile inside the resonator was calculated by software Psst (University of St Andrews, United Kingdom). According to this calculation the beam diameter in the crystal was approximately 600 μm and its diameter on the SA was 400 μm. In order to obtain better spatial overlap between the pump and smaller laser beam, a cylindrical focusing lens L1 (f = 50 mm) was used to focus the pumping radiation.

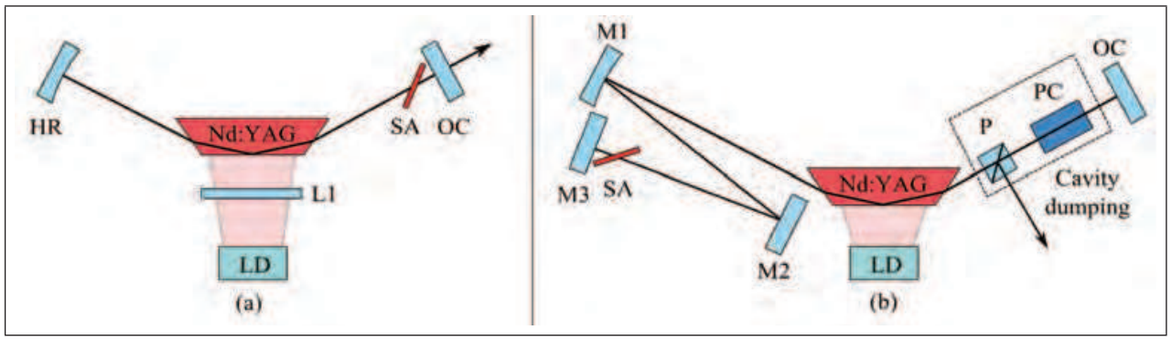

Fig. 7. Schematic of the laser in the mode-locked regime: oscillator (A) 250 mm long and oscillator (B) 1160 mm long.

The laser was passively mode-locked by a multiple quantum well semiconductor saturable absorbers (SA) inserted into the resonator close to the OC under the Brewster's angle in the transmission mode. Two different samples of saturable absorbers, consisted of 33 and 100 quantum wells (QW), were investigated. In addition its GaAs substrate served also as nonlinear element for passive negative feedback by beam defocusing.

Using the SA consisting 33 QW, the mode-locking threshold was achieved for pump energy of 17.5 mJ in 150 μs pulse. Pulse duration evolution along the train was measured by a fast oscilloscope LeCroy SDA 9000 and a PIN photodiode EOT ET-3500 and a typical output pulse train oscillogram together with details of the pulses at the beginning and the end of the train are shown in Fig. 8. The oscilloscope-photodiode system response time was 75 ps.

The measured pulse width was consequently recalculated using the experimentally determined oscilloscope-photodiode instrumental limit and *sum of square* method, which is in details described in Jelínek (2011c); Kubeček (2009d). Although the absolute calculated pulse duration may not be precise, pulse shortening from initial 120 ps to final 35 ps can be clearly observed and in summary is shown in Fig. 9. The whole train consisted of 100 pulses and its

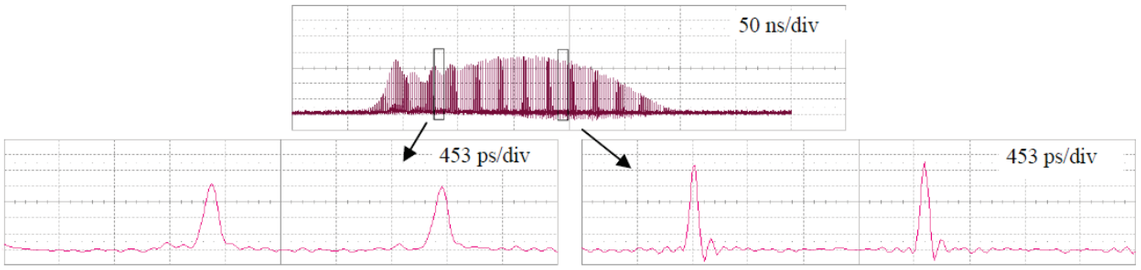

Fig. 8. Oscillogram of the output pulse train using the SA consisted of 33 QWs from the laser resonator (A) (250 mm long) - upper trace, and details of the pulse shapes from the beginning and the end of the train - lower traces.

energy was of 170 μJ. The output beam spatial profile was slightly elliptical in the horizontal axis but it was approximately Gaussian in both axes.

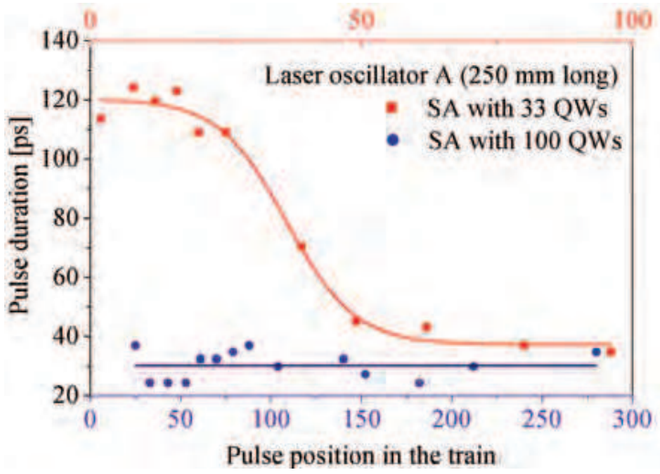

Fig. 9. Pulse duration evolution along the train for the laser resonator (A) mode-locked by the SA consisted of 33 and 100 quantum wells (QW).

Usage of the saturable absorber with 100 quantum wells resulted in higher mode-locking threshold (pump energy of 25 mJ in 180 μs pulse) and also to lengthening of the pulse train. The typical output pulse train oscillogram together with detail of the pulses in the middle of the train is shown in Fig. 10. In this case significant pulse shortening was not observed, the pulse duration of 30 ps remained at approximately constant value from the beginning along the whole train, as can be seen in Fig. 9. The whole train consisted of more than 300 pulses and its energy reached 500 μJ.

Using both saturable absorbers the extended pulse trains typical for passive negative feedback regime of operation were obtained. The corresponding pulse shortening along the train was observed only for pulses with initial pulse duration of 120 ps. With higher depth of modulation the shortening of initially 30 ps long pulses was not observed probably due to the limit of resolution of our detection system.

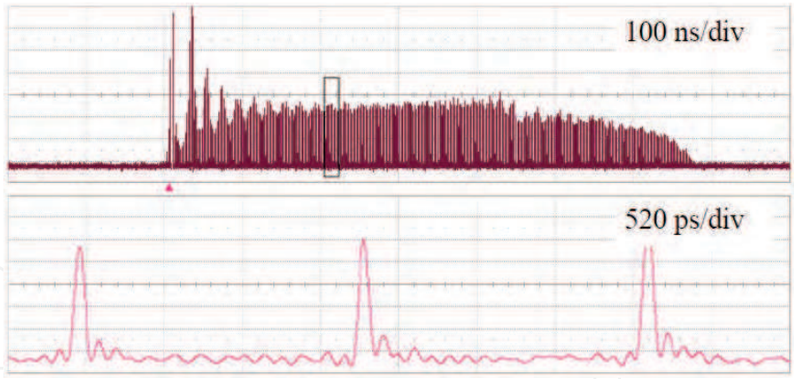

Fig. 10. Oscillogram of the output pulse train using the SA consisted of 100 QWs from the laser resonator A (250 mm long) - upper trace and details of the pulse shapes in the middle of the train - lower traces.

5.1.2 Laser operation with long resonator

In order to obtain shorter pulse trains with longer interval between pulses, which is necessary for cavity dumping, a longer resonator configuration was used. The experimental setup is in details described in Jelínek (2011b).

A schematic diagram of this investigated laser oscillator in configuration B is shown in Fig. 7b. The 116 cm long optical resonator was formed by a flat output coupler OC with the reflectivity of 30% at 1.06 μm, a high reflective folding mirror M1 with the radius of curvature of 1 m, a flat mirror M2, and a flat rear mirror M3. The laser was passively mode-locked by a multiple quantum well saturable absorber SA consisted of 100 quantum wells, inserted into the resonator under the Brewster's angle in transmission mode. The fundamental laser beam profile inside the crystal was approximately 1080 μm and its diameter on the SA was 640 μm.

The mode-locking operation threshold was obtained for the pump energy of 39 mJ in 270 μs long pulse. The output pulse train energy reached 900 μJ and its spatial profile was approximately Gaussian in both axes but slightly elliptical in the horizontal axis and is shown in the inset of Fig. 11. The train consisted of 7 pulses (at half-maximum) and the recorded oscillogram is shown in Fig. 11. Lower graphs show pulse duration histograms of the highest pulse (pulse no. 1) and the pulse no. 4. The Gaussian approximations of the histograms show only small decrease in the pulse duration from initial 76 to 69 ps. Increase in pulse duration stability is also observable, the Gaussian fit FWHM of the histogram decreased from 24 to 19 ps.

5.1.3 Single pulse extraction using cavity dumping

In order to obtain single mode-locked pulse, the cavity dumping technique was used. Into the resonator a KD*P Pockels cell PC and a Glan laser polarizer P were inserted. The radiation transmitted through the output coupler OC was used to trigger a high voltage generator supplying quarter wave step 4.8 kV signal (rise time below 7 ns) for the Pockels cell. The single pulse with the maximum amplitude from the train (pulse no. 1) was extracted with the energy of 30 μJ. In order to obtain maximum energy in the single pulse directly from the oscillator, the 50% output coupler was used. The pump energy of mode-locking operation

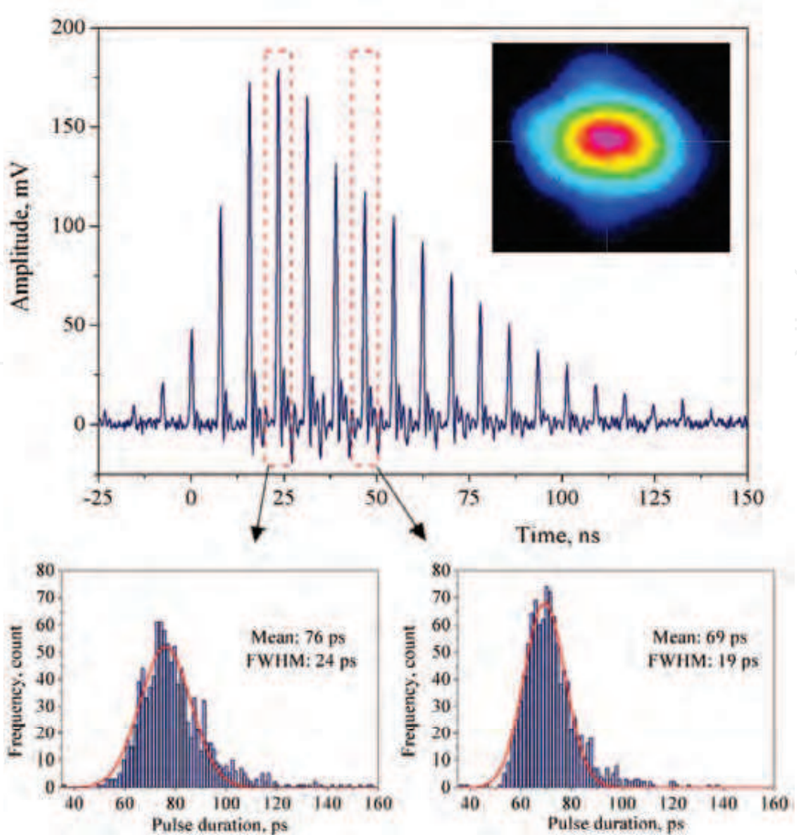

Fig. 11. Upper trace: oscillogram of the oscillator output pulse train. Lower traces: pulse duration histograms of the highest pulse (pulse no. 1) and the pulse no. 4.

threshold decreased to 26 mJ in 180 μs long pulse. The whole output train energy with this output coupler was 500 μJ (measured behind M1 without cavity dumping). The extracted single pulse energy increased to 75$\pm$7 μJ and the contrast was better than 10^{-3}. The pulse duration histogram was also measured and is shown in Fig. 12. Its Gaussian approximation gives the mean pulse duration of 113 ps. It can be seen that using the 50% output coupler the pulse duration is longer than using 30 % output coupler which corresponds to the lower saturated gain coefficient in the Nd:YAG.

5.2 Laser mode-locking by saturable absorber mirror

Simpler mode-locked laser configuration was obtained using a saturable absorber mirror (SAM) with high modulation depth. The experimental details and results listed below are in details described in Jelínek (2011d).

The laser oscillator schematic is shown in Fig. 13. The 112 cm long optical resonator was formed by a flat output coupler OC with reflectivity of 30 % at 1.06 μm, a highly reflective folding mirror M1 with the radius of curvature of 1 m, and a flat mirror M2. For passive mode-locking regime a commercially-available semiconductor anti-resonant saturable absorber mirror (SAM) with absorbance of 50 %, modulation depth of 25 %, and relaxation

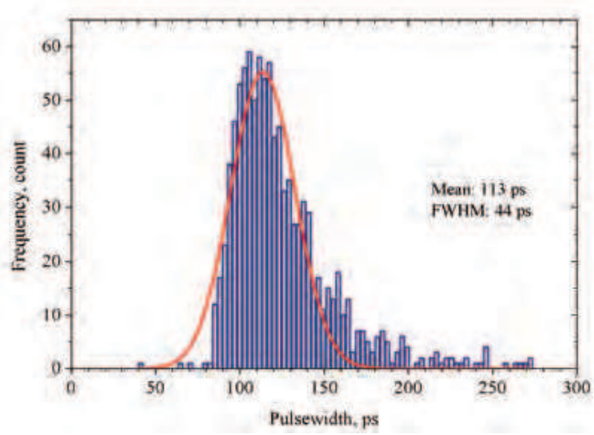

Fig. 12. Extracted pulse duration histogram.

time constant of 5 ps was used. The fundamental laser beam diameter was calculated to be approximately 1 mm in the Nd:YAG crystal and 700 μm on the SAM.

Stable mode-locked laser operation was obtained at the pump energy of 25 mJ in 180 μs long pulse. The 500 μJ output pulse train consisted of $\sim$ 15 pulses (at half-maximum) is shown in Fig. 14.

The output beam spatial profile was close to Gaussian in both axes and is shown in the inset of Fig. 14. Duration of the pulse with the maximum amplitude in the train was measured by the streak camera resulting in the value of 15 ps. The pulse duration stability measured from 10 successive laser shots was better than 2 ps and pulse train stretching was not observed. The duration of the pulse with maximum amplitude was also confirmed by the SHG autocorrelator. Assuming the Gaussian pulse shape the real pulse duration (measured from 1000 laser shots) was calculated to be 16 ps which is in the good agreement with the streak camera measurement. The streak camera and the autocorrelator records can be found in Jelínek (2011d).

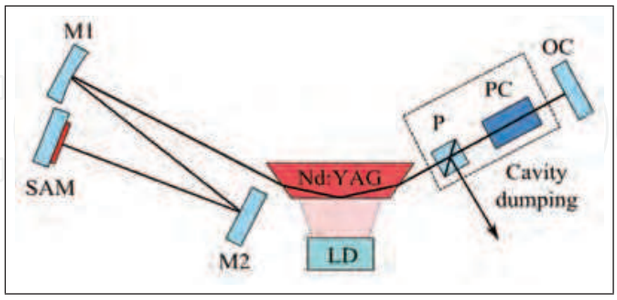

Fig. 13. Schematic of the Nd:YAG laser oscillator in the mode-locked regime using saturable absorber mirror (SAM).

5.2.1 Single pulse extraction using cavity dumping

A single pulse was extracted from the output pulse train by the cavity dumping technique, as it was described in section 5.1.3. In order to obtain high energy single pulse directly from

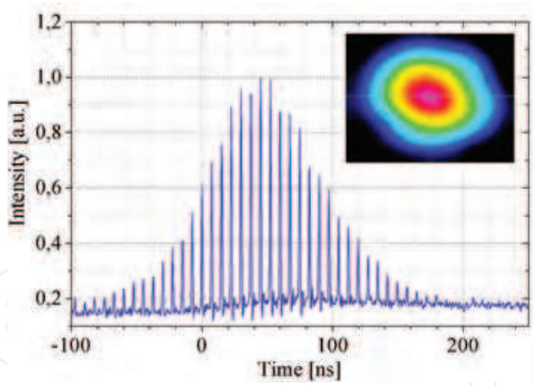

Fig. 14. Output pulse train without cavity dumping.

the oscillator, the output coupler with reflectivity of 70 % was used. Stable mode-locked laser operation was obtained at the pump energy of 19 mJ. Oscillogram of the output pulse train (measured behind the OC) and the extracted single pulse with energy of 25 μJ are shown in Fig. 15. The beam spatial profile was nearly Gaussian in both axes and is shown in the inset of the figure. Duration of the pulse was 17 ps with the stability better than 2 ps. The temporal profile measured by the streak camera is shown in Fig. 16. Inset shows the streak camera record of the pulse and its replica reflected from the 5 mm BK7 plate corresponding to the delay of 50 ps between pulses. In comparison with our previous results described in section 5.1.3, significant (about 5 times) pulse duration shortening and stability improvement was achieved.

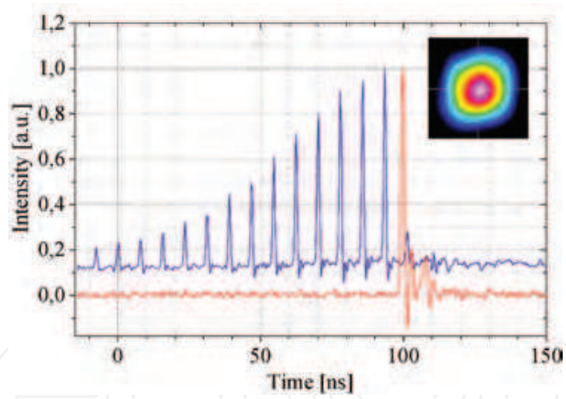

Fig. 15. Oscillogram of the ML Nd:YAG laser output pulse train (blue upper trace) and the extracted pulse (red lower trace).

6. Diode pumped Nd:YAG amplifier in bounce geometry

Performance of the Nd:YAG laser crystal in bounce geometry was also investigated in the single pass amplifier configuration and is in details described in Jelínek (2011a;b). The input pulse diameter was adjusted by a spherical lens to obtain good overlap with the pumped region. Several laser sources generating pulses in the range from 100 ps to 5 ns were used to provide the amplifier input fluence in the range from $\sim 1\,\mu\mathrm{J/cm^2}$ to $3\,\mathrm{J/cm^2}$. According to the laser source performance and certain amplifier setup the pump pulse duration ranging

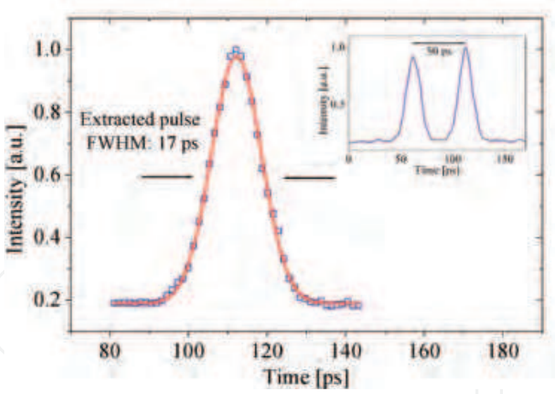

Fig. 16. Streak camera record of the ML Nd:YAG laser extracted pulse temporal profile (dots) and its Gaussian fit (red line).

from 200 to 300 μs with the energy from 29 to 42 mJ was used. Resulting amplification factor is shown in Fig. 17.

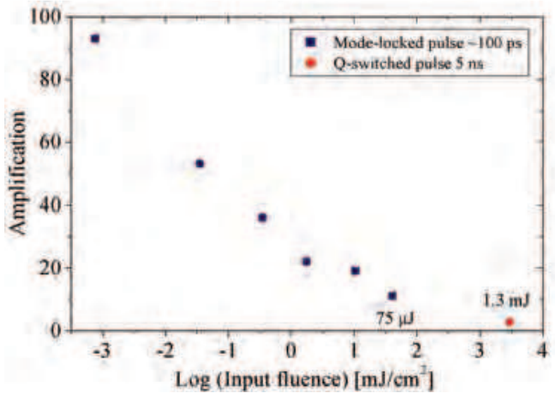

Fig. 17. Nd:YAG laser crystal in bounce geometry amplification under input fluence from 1 μJ/cm^2 to 3 J/cm^2.

It can be seen that in the weak signal regime ($\sim$ 1 μJ/cm^2), amplification up to 93 was obtained. In the strong signal regime (3 J/cm^2), the 1.3 mJ seed pulse was amplified to 3.5 mJ corresponding to the strong signal amplification about 3 times.

7. Conclusion

Operation of the highly 2.4 at.% doped Nd:YAG laser in bounce geometry under quasi-continuous pumping was investigated. The laser was operated in free-running, Q-switched and mode-locked regime. In the free-running regime, efficient operation at the wavelengths of 1.06, 1.3 and 1.4 μm was demonstrated with slope efficiencies of 50, 26, and 8 %, respectively. In the passively Q-switched regime at 1.06 μm, the 5 ns output pulses with the energy of 1.3 mJ were generated. At 1.34 μm, the 13 ns output pulses with energy of 600 μJ were generated.

In order to obtain passively mode-locked regime, two types of saturable absorbers inserted into the resonator either in the transmission or reflection mode were tested. Using the

saturable absorber with lower modulation depth (33 quantum wells) in the transmission mode, pulse duration shortening along the extended output pulse train from initial 120 to 35 ps was observed. Whole pulse train energy was 170 μJ. Using the saturable absorber with higher modulation depth (100 quantum wells), the 500 μJ train of 300 pulses with duration of 30 ps was generated without significant shortening effect. In order to be able to extract single pulse from the train, longer laser resonator was constructed. Using the cavity dumping technique, the single 75 μJ pulse with the duration of 113 ± 22 ps was extracted from the resonator.

Simpler mode-locked laser configuration was obtained using a saturable absorber mirror (SAM) with modulation depth of 25 %. The 500 μJ output pulse train consisted of 15 pulses with duration of 15 ps. By the cavity dumping technique, the single 25 μJ pulse with stable duration of 17 ps and Gaussian spatial profile was extracted from the resonator.

Single pass amplification using the Nd:YAG crystal in bounce geometry was also investigated in the weak and also strong signal regime. In the weak signal regime ($\sim 1\,\mu$J/cm^2), amplification up to 93 was obtained. In the strong signal regime (3 J/cm^2), the 1.3 mJ seed pulse was amplified to 3.5 mJ corresponding to the strong signal amplification about 3 times.

8. Acknowledgements

This research has been supported by the Czech Science Foundation under grant No. 102/09/1741, the research projects of the Czech Ministry of Education MSM 6840770022 "Laser Systems, radiation and modern optical applications" and ME 10131 "Picosecond solid state lasers and parametric oscillators for sensors of rotation and other physical quantities."

9. References

A. Agnesi, et al. (1994). Kerr-Lens Modelocking of Solid-State Lasers and Unidirectional Ring Cavities, *IEEE Journal of Quantum Electronics* 30: 1115-1121.

A. Agnesi, et al. (2008). 210-μJ picosecond pulses from a quasi-CW Nd:YVO_4 grazing-incidence two-stage slab amplifier package, *IEEE Journal of Quantum Electronics* 44: 952-957.

A. Agnesi and F. Pirzio (2010). High Gain Solid-State Amplifiers for Picosecond Pulses, in M. Grishin (ed.), *Advances in Solid-State Lasers: Development and Applications*, Intech, Croatia, pp. 213-238.

A. Alcock and J. Bernard (1992). Diode-pumped grazing incidence slab lasers, *IEEE J. Sel. Top. Quantum Electronics* 3: 3-8.

A. D. Corno, et al. (1990). Active-passive mode-locked Nd:YAG laser with passive negative feedback, *Optics Letters* 15: 734-736.

J. Cui, et al. (2009). 500 W Nd:YAG zigzag slab MOPA laser, *Laser Physics* 19: 1974-1976.

J.-C. Diels and W. Rudolph (2006). *Ultrashort Laser Pulse Phenomena*, Elsevier, USA.

J. Dong, et al. (2005). Temperature-dependent stimulated emission cross section and concentration quenching in highly doped Nd^{3+}:YAG crystals, *Phys. stat. sol.* 202: 2565-2573.

X. Fu, et al. (2010). 1 mJ, 500 kHz Nd:YAG/Nd:YVO_4 MOPA laser with a Nd:YAG cavity-dumping seed laser, *Laser Physics* 20: 1707-1711.

X. Fu, et al. (2009). 120W high repetition rate Nd:YVO_4 MOPA laser with a Nd:YAG cavity-dumped seed laser, *Applied Physics B* 95: 63–67.
S. Gupta, et al. (1992). Ultrafast Carrier Dynamics in III-V Semiconductors Grown by Molecular-Beam Epitaxy at Very Low Substrate Temperatures, *IEEE Journal of Quantum Electronics* 28: 2464-2472.
M. Jelínek, et al. (2010). Passively mode locked quasi-continuously pumped 2.4% doped crystalline Nd:YAG laser in a bounce geometry, *Proc. SPIE* 7721: 772115.
M. Jelínek, et al. (2011a). Passively Q-switched quasi-continuously pumped 2.4% Nd:YAG laser in a bounce geometry, *Proc. SPIE* 7912: 791221.
M. Jelínek, et al. (2011b). 0.8 mJ quasi-continuously pumped sub-nanosecond highly doped Nd:YAG oscillator-amplifier laser system in bounce geometry, *Laser Physics Letters* 8: 205-208.
M. Jelínek, et al. (2011c). Single shot diagnostics of quasi-continuously pumped picosecond lasers using fast photodiode and digital oscilloscope, in J.-W. Shi (ed.), *Photodiodes - Communications, Bio-Sensings, Measurements and High-Energy Physics*, Intech, Croatia.
M. Jelínek and V. Kubeček (2011d), 15 ps quasi-continuously pumped passively mode-locked highly doped Nd:YAG laser in bounce geometry, *Laser Physics Letters* 8: 657-660.
U. Keller, et al. (1996). Semiconductor saturable absorber mirrors (SESAMS) for femtosecond to nanosecond pulse generation in solid-state lasers, *IEEE J. Sel. Top. Quantum Electronics* 2: 435-453.
W. Koechner (2006). *Solid-state laser engineering*, Springer, USA.
V. Kubeček, et al. (2008). Side pumped Nd:YAG slab laser mode-locked using multiple quantum well saturable absorbers, *Laser Phys. Letters* 5: 29-33.
V. Kubeček, et al. (2009a). Quasi-continuously pumped passively mode-locked operation of a Nd:$GdVO_4$ and Nd:YVO_4 laser in a bounce geometry, *Laser Physics* 19: 396-399.
V. Kubeček, et al. (2009b). Quasi-continuously pumped operation of 2.4% doped crystalline Nd:YAG in a bounce geometry, *Proc. SPIE* 7193: 719320.
V. Kubeček, et al. (2009c). Quasi-Continuously Pumped Passively Mode-Locked Operation of a Nd:$GdVO_4$ and Nd:YVO_4 Laser in a Bounce Geometry, *Laser Physics* 19: 396-399.
V. Kubeček, et al. (2009d). Pulse shortening by passive negative feedback in mode-locked train from highly-doped Nd:YAG in a bounce geometry, *Proc. SPIE* 7354: 73540R.
V. Kubeček, et al. (2010). 0.4 mJ quasi-continuously pumped picosecond Nd:$GdVO_4$ laser with selectable pulse duration, *Laser Physics Letters* 7: 130-134.
C.-C. Lee, et al. (2010) Ultra-short optical pulse generation with single-layer graphene, *Journal of Nonlinear Optical Physics and Materials* 19: 767-771.
M. Luhrmann, et al. (2009). High energy cw-diode pumped Nd:YVO_4 regenerative amplifier with efficient second harmonic generation, *Optics Express* 17: 22761-22766.
D. Sauder, et al. (2006). High efficiency laser operation of 2at.% doped crystalline Nd:YAG in a bounce geometry, *Opt. Express* 14: 1079-1085.
D. Sauder, et al. (2007). Laser operation at 1.3 μm of 2at.% doped crystalline Nd:YAG in a bounce geometry, *Opt. Express* 15: 3230-3235.
F. P. Schafer, et. al. (1976). Organic dyes in laser technology, *Topics in Current Chemistry* 61.
K. A. Stankov (1988). A Mirror with an Intensity-Dependent Reflection Coefficient, *Appl. Phys. B* 45: 191-195.
D. E. Spence, et. al. (1991). 60-fsec pulse generation from a self-mode-locked Ti:sapphire laser, *Optics Letters* 16: 42-44.

W. D. Tan, et. al. (2010). Mode locking of ceramic Nd:yttrium aluminum garnet with graphene as a saturable absorber, *Applied Physics Letters* 96: 031106.

G. M. Thomas, et al. (2010). Nonlinear mirror modelocking of a bounce geometry laser, *Optics Express* 18: 12663-12668.

Y. Urata, et al. (2001). Laser performance of highly neodymium-doped yttrium aluminum garnet crystals, *Opt. Letters*, 26: 801–803.

X. Wushouer, et al. (2010). High peak power picosecond hybrid fiber and solid-state amplifier system, *Laser Phys. Letters* 7: 644-649.

J. H. Yim, et al. (2008). Fabrication and characterization of ultrafast carbon nanotube saturable absorbers for solid-state laser mode locking near 1 μm, *Applied Physics Letters*, 93: 161106.

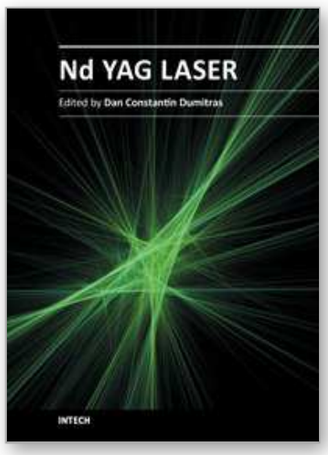

Nd YAG Laser

Edited by Dr. Dan C. Dumitras

ISBN 978-953-51-0105-5
Hard cover, 318 pages
Publisher InTech
Published online 02, March, 2012
Published in print edition March, 2012

Discovered almost fifty years ago at Bell Labs (1964), the Nd:YAG laser has undergone an enormous evolution in the years, being now widely used in both basic research and technological applications. Nd:YAG Laser covers a wide range of topics, from new systems (diode pumping, short pulse generation) and components (a new semiorganic nonlinear crystal) to applications in material processing (coating, welding, polishing, drilling, processing of metallic thin films), medicine (treatment, drug administration) and other various fields (semiconductor nanotechnology, plasma spectroscopy, laser induced breakdown spectroscopy).

How to reference

In order to correctly reference this scholarly work, feel free to copy and paste the following:

Michal Jelínek and Václav Kubeček (2012). Highly Doped Nd:YAG Laser in Bounce Geometry Under Quasi-Continuous Diode Pumping, Nd YAG Laser, Dr. Dan C. Dumitras (Ed.), ISBN: 978-953-51-0105-5, InTech, Available from: http://www.intechopen.com/books/nd-yag-laser/highly-doped-nd-yag-laser-in-bounce-geometry-under-quasi-continuous-diode-pumping

INTECH
open science | open minds

InTech Europe
University Campus STeP Ri
Slavka Krautzeka 83/A
51000 Rijeka, Croatia
Phone: +385 (51) 770 447
Fax: +385 (51) 686 166
www.intechopen.com

InTech China
Unit 405, Office Block, Hotel Equatorial Shanghai
No.65, Yan An Road (West), Shanghai, 200040, China
中国上海市延安西路65号上海国际贵都大饭店办公楼405单元
Phone: +86-21-62489820
Fax: +86-21-62489821

IntechOpen